

## Supplementary Material

### **Co<sub>2</sub>(P<sub>4</sub>O<sub>12</sub>)/CoSe<sub>2</sub> heterostructures grown on carbon nanofibers as an efficient electrocatalysts for water splitting**

Wenjing Cui<sup>a,b</sup>, Xingwei Sun<sup>\*a,b</sup>, Shaoshuai Xu<sup>a,b</sup>, Chunping Li<sup>\*a,b</sup>, Jie Bai<sup>a,b</sup>

<sup>a</sup>Chemical Engineering College, Inner Mongolia University of Technology,  
Hohhot, 010051, People's Republic of China

<sup>b</sup>Inner Mongolia Key Laboratory of Industrial Catalysis, Hohhot, 010051,  
People's Republic of China

\*Corresponding authors: Xingwei Sun, Chunping Li

Tel: +86471 6575722.

Fax: +86471 6575722.

E-mail address: [sxw@imut.edu.cn](mailto:sxw@imut.edu.cn), [hgcp\\_li@126.com](mailto:hgcp_li@126.com)

## 1. Experimental details

### 1.1 Materials and reagents

Cobalt nitrate hexahydrate ( $\text{Co}(\text{NO}_3)_2 \cdot 6\text{H}_2\text{O}$ , 99% Aladdin Reagent). Selenium powder (Se, 99.99%) was obtained from Anhui Senrise Technology Co., Ltd. Sodium hypophosphite ( $\text{NaH}_2\text{PO}_2$ , AR, 99% Aladdin Reagent). Polyacrylonitrile (PAN, Mw = 80, 000) was provided by Kunshan Hongyu Plastics Co., Ltd. 2-Methylimidazole ( $\text{C}_4\text{H}_6\text{N}_2$  GR, 98% McLean Reagent) and methyl alcohol ( $\text{CH}_3\text{OH}$ , AR, 99.5%) were obtained from Sinopharm Chemical Reagent Co., Ltd. Potassium hydroxide (KOH, GR, 99.5%) and N, N-Dimethylformamide (DMF, AR, 99.5%) were purchased from Fuchen (Tianjin) Chemical Reagent Co., Ltd. Nickel foam (NF, GR, 99.9% Alfa Aesar Reagent). All of these chemical reagents were used with further purification.

### 1.2 Preparation process

Dissolve 1 g PAN in 9 g DMF, add 0.0774 g 2-MI, and electrospinning to obtain the 2-MI/PAN nanofiber membrane.  $\text{Co}(\text{NO}_3)_2 \cdot 6\text{H}_2\text{O}$  (0.8187 g) was dissolved in 30 mL of methanol, and 0.02 g 2-MI/PAN fiber membrane was immersed in the above solution for 36 h. Finally, the fiber membrane was further immersed in a 25 mL methanol solution containing 2-MI (0.4561 g) and  $\text{Co}(\text{NO}_3)_2 \cdot 6\text{H}_2\text{O}$  (0.0909 g) for 24 h, at room temperature. Finally, wash with methanol and dry for 12 h. The ZIF-67/PAN fiber membrane was stabilized at 200°C for 2 h at a heating rate of 5°C min<sup>-1</sup> in air atmosphere, and further stabilized at 850°C for 2 h at a heating rate of 2°C min<sup>-1</sup> in N<sub>2</sub> atmosphere, resulting in the final product of CoO<sub>x</sub>/CNFs.

Place CoO<sub>x</sub>/CNFs downstream of the tube furnace, and place Se powder and NaH<sub>2</sub>PO<sub>2</sub> upstream (in a mass ratio of 1:1). Under N<sub>2</sub> atmosphere, phosphorus and selenium were treated at 5 °C min<sup>-1</sup> heating rate for 2 h at 500°C. The final product was a heterostructure of Co<sub>2</sub>(P<sub>4</sub>O<sub>12</sub>) and CoSe<sub>2</sub>, named Co<sub>2</sub>(P<sub>4</sub>O<sub>12</sub>)/CoSe<sub>2</sub>/CNFs-2. By changing the mass ratio of Se powder and NaH<sub>2</sub>PO<sub>2</sub> (1:3 and 3:1), two materials were obtained, named Co<sub>2</sub>(P<sub>4</sub>O<sub>12</sub>)/CoSe<sub>2</sub>/CNFs-1 and Co<sub>2</sub>(P<sub>4</sub>O<sub>12</sub>)/CoSe<sub>2</sub>/CNFs-3, respectively. In addition, the preparation method of Co<sub>2</sub>(P<sub>4</sub>O<sub>12</sub>)/CNFs and CoSe<sub>2</sub>/CNFs was consistent with that of the heterostructure, except for the last step of not adding Se powder/NaH<sub>2</sub>PO<sub>2</sub>.

### 1.3. Electrochemical measurements

### 1.3.1. Methods for preparing OER and HER catalysts and electrochemical testing

Catalyst preparation: Grind the prepared composite material into a powder, take 1 mg of it, add 1 mL of deionized water, 0.98 mL of ethanol, and 2  $\mu\text{L}$  of Nafion solution (5%wt) in sequence, and ultrasonicate the catalyst ink at a frequency of 40 Hz for 10 minutes. Drop 150  $\mu\text{L}$  of the catalyst ink onto the carbon paper at a loading of 0.5  $\text{cm}^{-2}$  and let it dry naturally for use.

Test method: The test was conducted using a CS350 electrochemical workstation. Before the test, the solution was saturated with 99.9%  $\text{O}_2$  (OER) or  $\text{N}_2$  (HER) for 30 minutes in 1 M KOH electrolyte solution. In the three-electrode system, a graphite rod was used as the counter electrode, a Hg/HgO electrode was used as the reference electrode, and a carbon paper loaded with catalyst was used as the working electrode for the test. First, the working electrode was activated by performing 50 cycles of linear cyclic voltammetry (CV) at a scan rate of 100  $\text{mV s}^{-1}$ . Then, the linear sweep voltammetry (LSV) curve was tested at a scan rate of 5  $\text{mV s}^{-1}$ . The electrical impedance (EIS) test range was 0.01-10<sup>5</sup> Hz. The electrical active area (ECSA) was calculated from the CV curve measured in the non-Faraday interval. The stability was tested using the CV cycling method. The reversible hydrogen electrode potential was calculated from the Hg/HgO electrode potential according to the Nernst equation as follows:

$$E_{\text{RHE}} = E_{\text{Hg/HgO}} + 0.0592\text{pH} + 0.098 \text{ V} \quad (1-1)$$

Among them,  $E_{\text{RHE}}$  is the potential of the reversible hydrogen electrode (RHE),  $E_{\text{Hg/HgO}}$  is the potential of the Hg/HgO electrode, and pH is the pH value of the electrolyte.

### 1.3.2. Assembly and electrochemical testing of a fully aqueous battery

The preparation of OER and HER catalysts is the same. Finally, the catalyst ink is dropped onto the surface of the carbon paper to form a circular shape with a radius of 0.5 cm (the loading amount is about 2.0  $\text{mg cm}^{-2}$ ). Using 1 M KOH as the electrolyte, the carbon paper loaded with the catalyst is used as the anode and cathode to assemble a water electrolysis cell. First, the material is subjected to 50 cycles of CV test at a sweep speed of 100  $\text{mV s}^{-1}$ ; then, the polarization curves are obtained by LSV at a sweep speed of 5  $\text{mV s}^{-1}$ ; the stability is tested by i-t test.

## 1.4. Materials characterization

The morphologies and structures of the samples were acquired by using the

scanning electron microscopy (SEM, Pro, Phenom, Netherlands) and transmission scanning electron microscopy (TEM, JEM-2100 (JEOL, Japan). The X-ray diffraction (XRD, Rigaku Ultima IV, Japan ) using a Cu Ka radiation ( $\lambda = 0.15406$  nm) was used to analyst crystallization characteristics. The surface chemical composition and chemical Valence were identified by X-ray photoelectron spectroscopy (XPS, Escalab 250xi, Thermo Fisher Scientific USA). Using an argon laser ( $\lambda = 532$  nm) excitation source to record Raman spectra (InVia Microscope Raman, Renishaw, England). The structure of the samples was characterized by Fourier transform infrared spectroscopy (FTIR, is50, Thermo Fisher Scientific USA).The scan wavenumber range was 500-4000  $\text{cm}^{-1}$ . The thermal decomposition behavior of the samples was characterized by thermal analyzer (TG, STA449F3, Netzsch Corporation of Germany).The samples were heated to 700 °C at a rate of 10 °C/min in an air atmosphere.

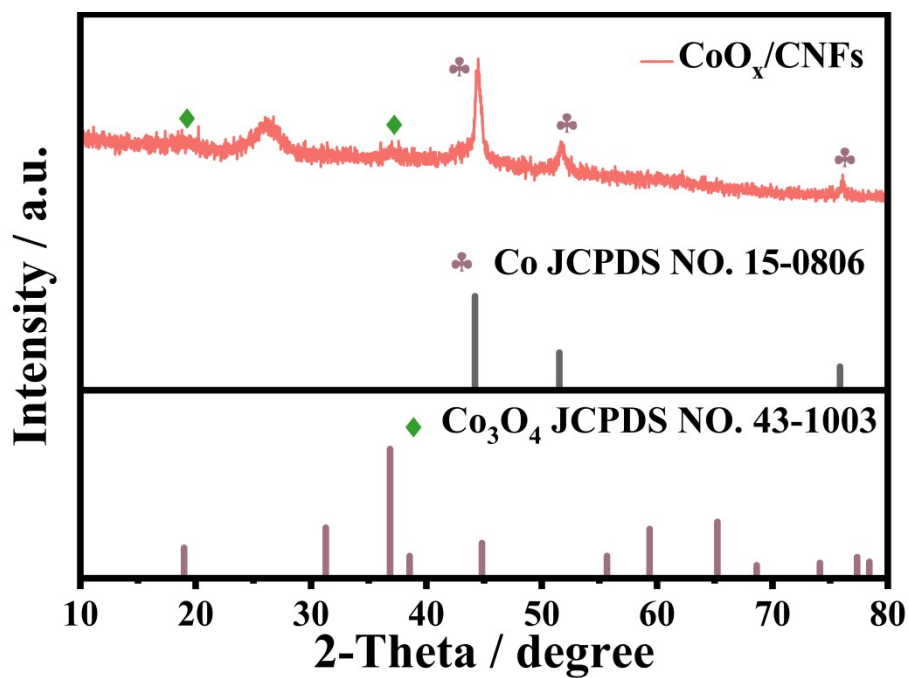


Fig. S1 XRD patterns of CoO<sub>x</sub>/CNFs

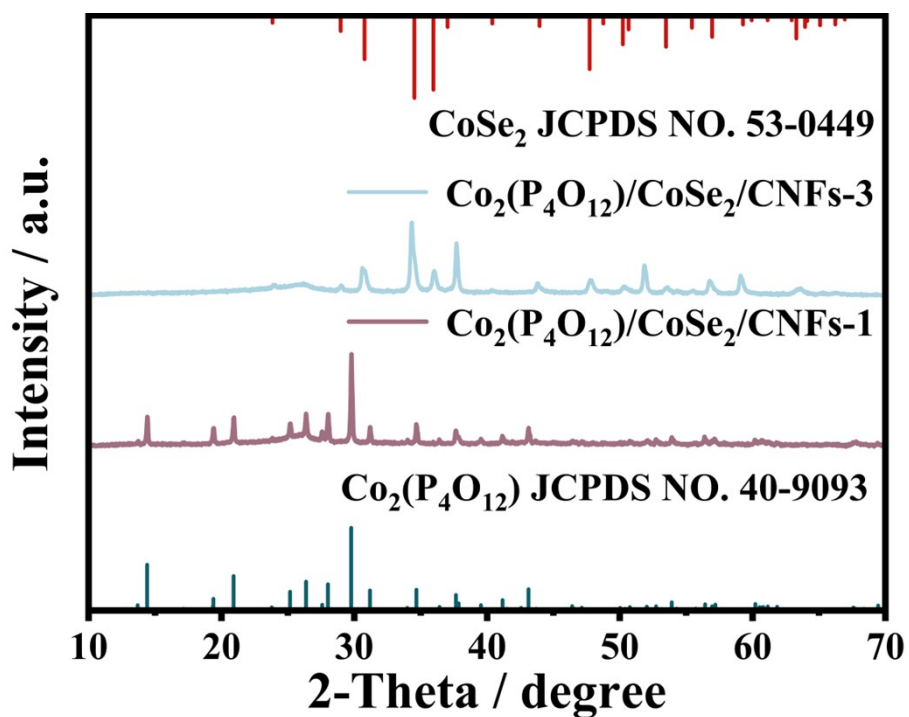


Fig. S2 XRD patterns of Co<sub>2</sub>(P<sub>4</sub>O<sub>12</sub>)/CoSe<sub>2</sub>/CNFs-3 and Co<sub>2</sub>(P<sub>4</sub>O<sub>12</sub>)/CoSe<sub>2</sub>/CNFs-1

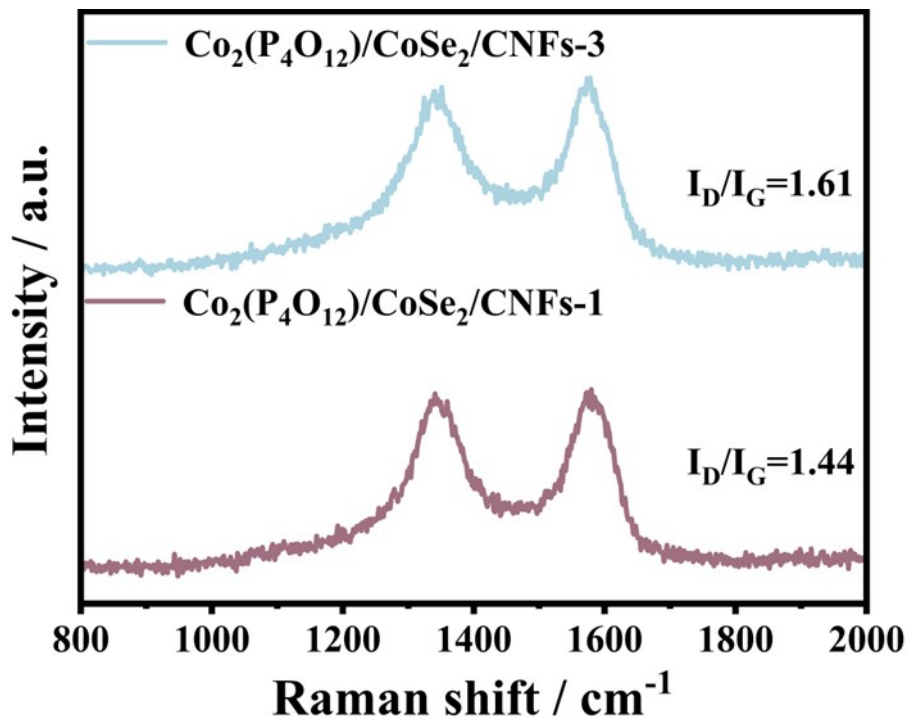


Fig. S3 Raman spectra of  $\text{Co}_2(\text{P}_4\text{O}_{12})/\text{CoSe}_2/\text{CNFs-3}$  and  $\text{Co}_2(\text{P}_4\text{O}_{12})/\text{CoSe}_2/\text{CNFs-1}$

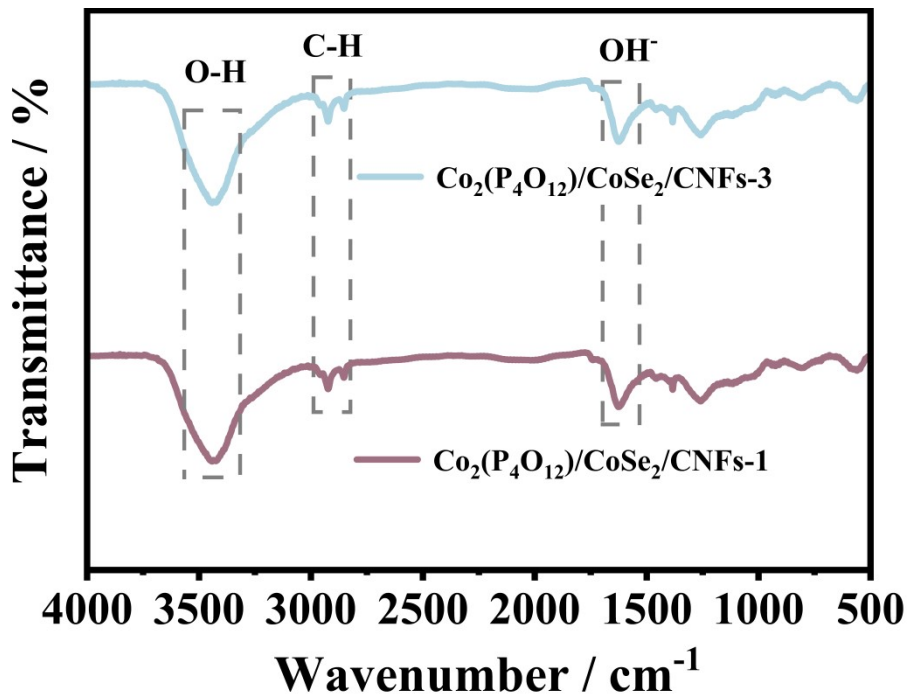


Fig. S4 FTIR spectra of  $\text{Co}_2(\text{P}_4\text{O}_{12})/\text{CoSe}_2/\text{CNFs-3}$  and  $\text{Co}_2(\text{P}_4\text{O}_{12})/\text{CoSe}_2/\text{CNFs-1}$

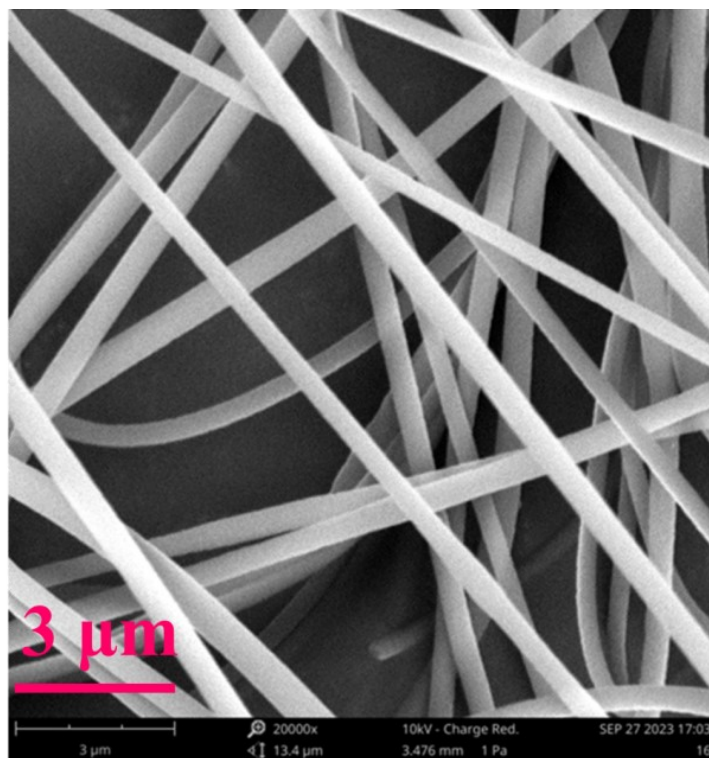


Fig. S5 SEM images of 2-MI/PAN

Table S1 Comparison of the OER performance of different catalysts

Catalyst	$E_{\text{OER}@10 \text{ mA cm}^{-2}}$ (V vs. RHE)	Reference
$\text{Co}_2(\text{P}_4\text{O}_{12})/\text{CoSe}_2/\text{CNFs-2}$	315	This work
CoSe/MoSe <sub>2</sub>	350	[1]
CoSe <sub>2</sub> /CoNC	380	[2]
CoSe <sub>2</sub> @CoNi LDH HNA	350	[3]
CoP-HNTs@NCL-0.4	350	[4]
Ru-CoP/NC	330	[5]
CoP@NC/NCNT	324	[6]

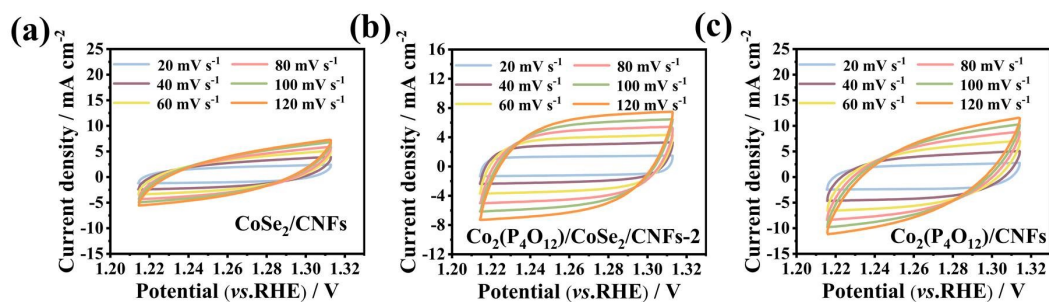


Fig. S6 The CV curves of (a)  $\text{CoSe}_2/\text{CNFs}$ , (b)  $\text{Co}_2(\text{P}_4\text{O}_{12})/\text{CoSe}_2/\text{CNFs-2}$  and (c)  $\text{Co}_2(\text{P}_4\text{O}_{12})/\text{CNFs}$  at different scan rates

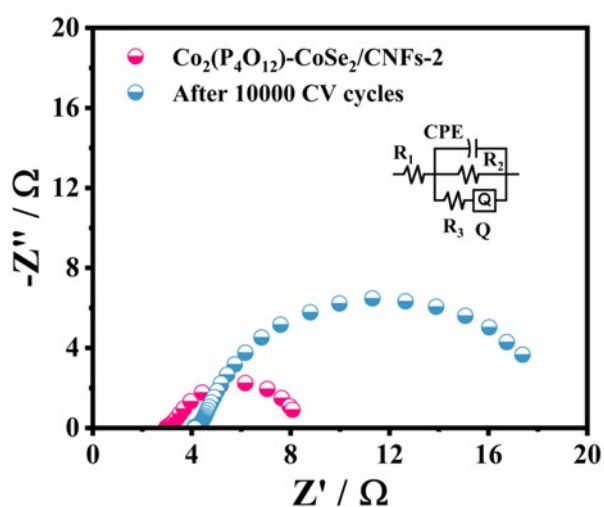


Fig. S7. The EIS data before and after the OER stability test of  $\text{Co}_2(\text{P}_4\text{O}_{12})/\text{CoSe}_2/\text{CNFs-2}$

Table S2 Comparison of the HER performance of different catalysts

Catalyst	$E_{\text{HER}}@10 \text{ mA cm}^{-2}$ (V vs. RHE)	Referenc e
$\text{Co}_2(\text{P}_4\text{O}_{12})/\text{CoSe}_2/\text{CNFs-2}$	221	This work
CoP/CNFs	225	[7]
Ni-CoSe <sub>2</sub> /BCT	250	[8]
CoSe <sub>2</sub> /CC	243	[9]
CNT@CoP	235	[10]
CoP-SSM	266	[11]



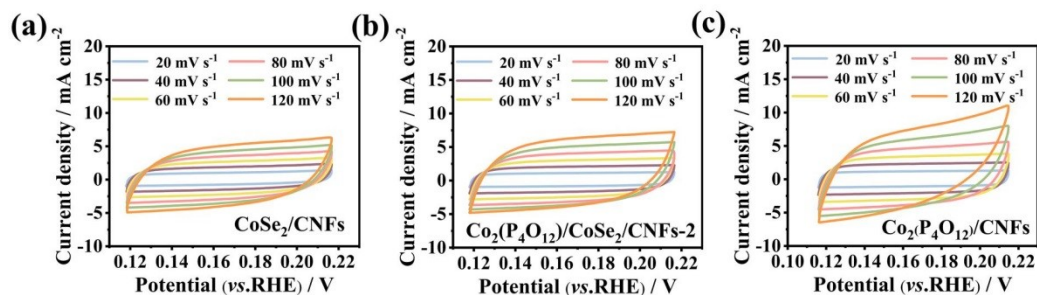


Fig. S8 The CV curves of (a)  $\text{CoSe}_2/\text{CNFs}$ , (b)  $\text{Co}_2(\text{P}_4\text{O}_{12})/\text{CoSe}_2/\text{CNFs-2}$  and (c)  $\text{Co}_2(\text{P}_4\text{O}_{12})/\text{CNFs}$  at different scan rates

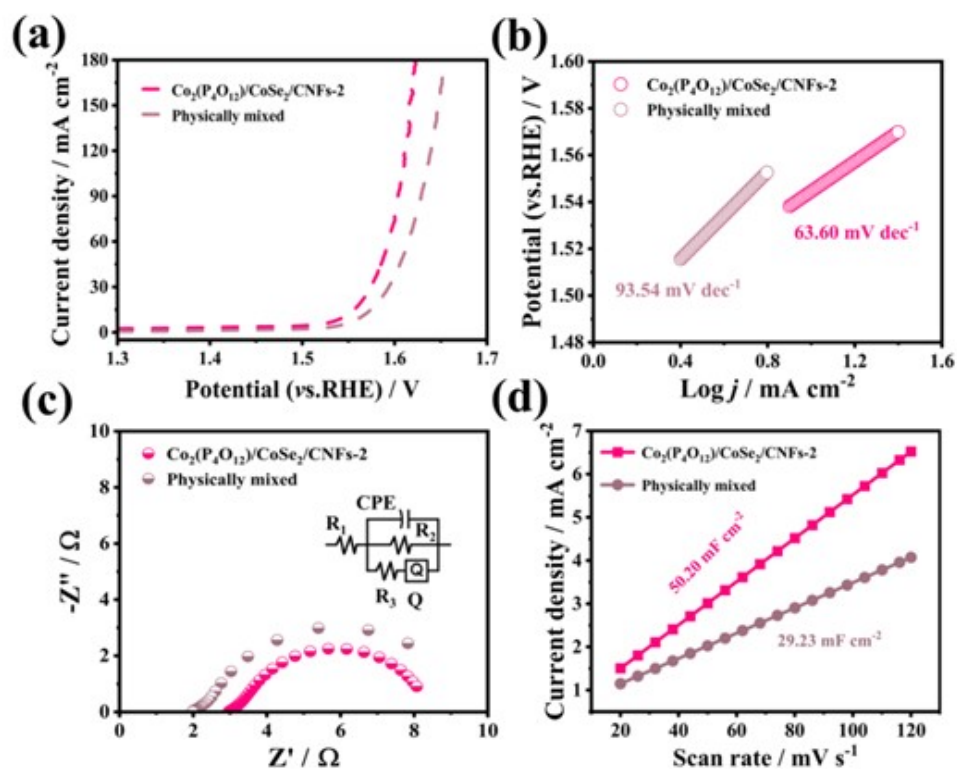


Fig. S9. (a) OER polarization curves, (b) Tafel plots, (c) Nyquist plots and fit the circuit diagram, (d) Electrochemical double-layer capacitance of  $\text{Co}_2(\text{P}_4\text{O}_{12})/\text{CoSe}_2/\text{CNFs-2}$  and physical mixed catalyst

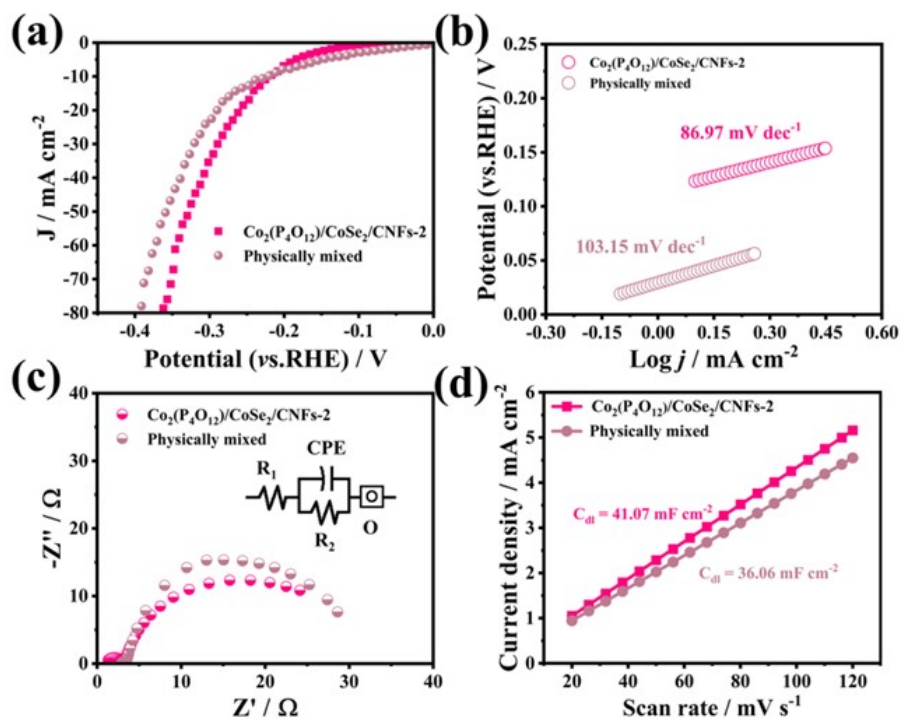


Fig. S10. (a) HER polarization curves, (b) Tafel plots, (c) Nyquist plots and fit the circuit diagram, (d) Electrochemical double-layer capacitance of  $\text{Co}_2(\text{P}_4\text{O}_{12})/\text{CoSe}_2/\text{CNFs-2}$  and physical mixed catalyst

Table S3 Comparison of the OWS performance of different catalysts

Catalyst	Voltage at $10 \text{ mA cm}^{-2}$ (V)	Reference
$\text{Co}_2(\text{P}_4\text{O}_{12})/\text{CoSe}_2/\text{CNFs-2}$	1.71	This work
$\text{CoP}_4/\text{FeP}_4$	1.74	[13]
$\text{CoSe}_2/\text{CMF}$	1.85	[14]
$\text{CoP}/\text{Graphene}$	1.73	[15]
$\text{h-CoP@NC-900-300}$	1.76	[16]
$\text{CoSe}_2/\text{CNTs}$	1.75	[17]

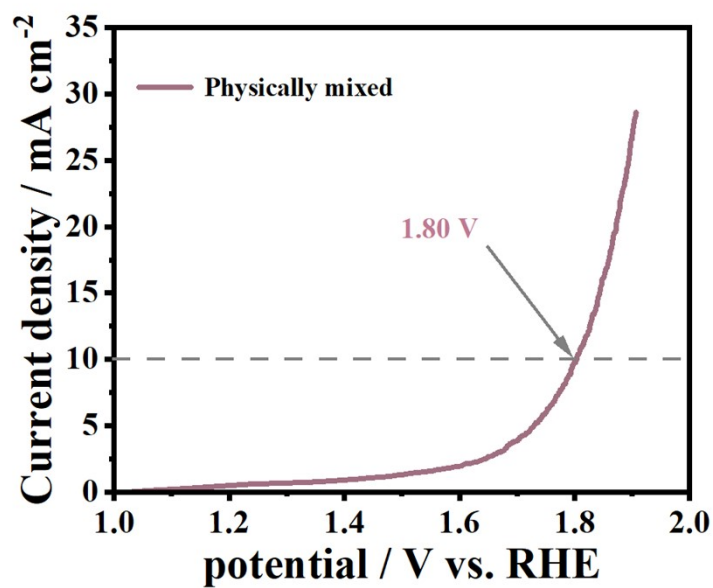


Fig. S11. LSV curve of water splitting of physical mixed catalyst

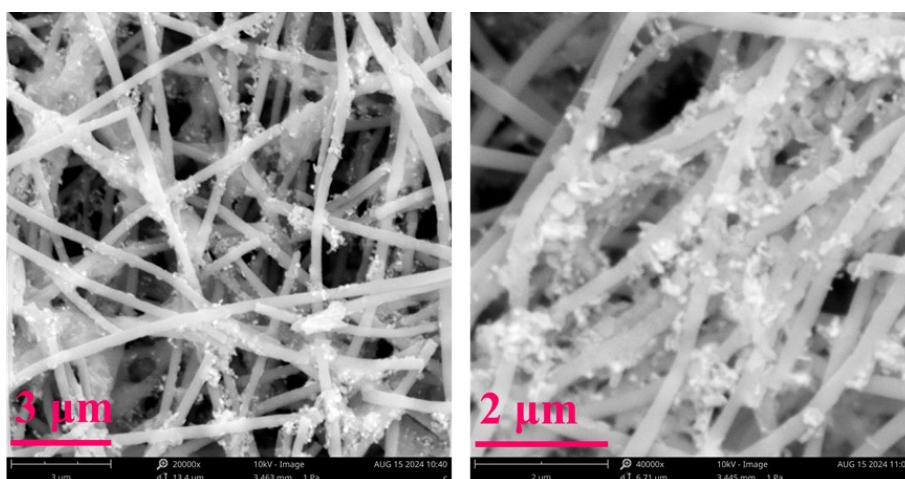


Fig. S12 SEM images of  $\text{Co}_2(\text{P}_4\text{O}_{12})/\text{CoSe}_2/\text{CNFs-2}$  electrode material after water splitting stability

## References

- [1] J. P. Sun, J. Li and Z. Z. Li, ACS Sustain Chem Eng. 2022, 10, 9980-9990.
- [2] K. Q. Li, R. Q. Cheng and Q. Y. Xue, Chem. Eng. J. 2022, 450, 137991.
- [3] J. N. Song, Y. Chen and H. J. Huang, Adv. Sci. 2022, 9, 2104522.
- [4] B. Liu, R. Y. Wang and Y. Yao, Chem. Eng. J. 2022, 431, 133238.

- [5] Y. R. Hao, H. Xue and J. Sun, *ACS Appl. Mater. Interfaces*. 2021, 13, 56035-56044.
- [6] Z. D. Wu, B. Y. Liu and H. Y. Jing, *J. Colloid Interface Sci.* 2023, 629, 22-32.
- [7] X. Q. Xie, J. P. Liu and C. N. Gu, *J. Energy Chem.* 2022, 64, 503-510.
- [8] G. Yang, Y. F. Zhang and J. P. Liu, *Int. J. Hydrogen Energy*. 2022, 47, 38920-38929.
- [9] Y. Wang, X. Y. Sun and Y. Liu, *Fuel*. 2024, 357, 129825.
- [10] C. L. Zhang, Y. Xie and J. T. Liu, *Chem. Eng. J.* 2021, 419, 129977.
- [11] A. F. Alharbi, A. A.M. Abahussain and W. Wazeer, *Int. J. Hydrogen Energy*. 2023, 48, 31172-31186.
- [12] T. Wang, C. C. Jia and B. Wang, *J. Alloys Compd.* 2020, 813, 152211.
- [13] H. L. Yan, X. Xiao and X. H. Liu, *Int J Hydrogen Energ.* 2022, 47, 23230-23239.
- [14] Y. X. Wang, J. Yu and Q. Liu, *Electrochim Acta.* 2023, 438, 141594.
- [15] L. Li, X. R. Wang and Y. Guo, *Langmuir*. 2021, 36, 1916-1922.
- [16] X. Z. Song, Y. H. Zhao and W. B. Yang, *ACS Appl. Nano Mater.* 2021, 4, 13450-13458.
- [17] G. J. Wei, K. Du and X. X. Zhao, *Chin. Chem. Lett.* 2020, 31, 2641-2644.